Asian Journal of Chemistry; Vol. 33, No. 10 (2021), 2333-2340

ASIAN JOURNAL OF CHEMISTRY

https://doi.org/10.14233/ajchem.2021.23298

Physico-Chemical Studies of Almond Shell Extracts Potential on the Electropolishing and Electrorefining of Copper

FATMA M. ABOUZEID*, and SULTANAH ALSHAMMERY

Department of Basic Science, Imam Abdulrahman bin Faisal University, Dammam, Kingdom of Saudi Arabia

*Corresponding author: Tel: +966 507555821; E-mail: fmabouzeid@iau.edu.sa

Received: 11 May 2021; *Accepted*: 13 July 2021; *Published online*: 20 September 2021; AJC-20503

Addition of almond shell extract to electrochemical process bath such as electropolishing and electrorefining of copper was investigated using potentiodynamic polarization and surface investigation. Addition of several concentrations of the extracts provide a sharp decline in electrorefining rate, but gave augmentation in electropolishing rate. Surfce investigation provided the confirmatory evidence of improved surface texture by almond shell extract addition to copper electropolishing and electrorefining electrolyte. Kinetic investigation and activated constraints were calculated for the electrochemical processes. A distinct improvement in the surface texture was observed where surface irregularity, roughness (Ra) diminishs from 0.95 to 0.43, 0.32, 0.22 and 0.06 μm in the presence of 25, 100, 150 and 200 ppm extract.

Keywords: Electropolishing, Electrorefining, Copper, Almond shell extract, Scanning electron microscopic, Surface roughness.

INTRODUCTION

Metallic anodes are widely used in the electrochemical industries. An anode must dissolve with simultaneous smoothing and brightening of the surface (electropolishing). Electropolishing is surface finishing ocure *via* chemical technique through which metal surface ion by ion is removed electrically. The main purpose is to diminish the metal microroughness. Hence considerably dipping the product dust remains or sticking and enhancing the surface cleanability. Electropolishing is also used for brightening and passivating [1,2]. The major electropolishing motive inserts is soft and silky surface production and make an inactive coating of oxide to diminish the deterioration rate; electropolishing also eases outstanding pressure. Precise electrolytes formulations are essential for alloys and metals electropolishing [3,4].

The dissolution of anodes must be selective, *i.e.* one of the components of the anode material is to dissolve quantitatively (often in the form of definite ions), while the others must not dissolve at all. An example is the electrolytic refining of copper. In this process, copper dissolves as cupric ions, while noble metals remain intact and accumulate at the bottom of the bath in the form of sludge [5].

The victorious accomplishment for copper electroplating expertise in the electronic devices metallization obtained from the electrolyte preservatives use to influence the local deposition rate [6]. This procedure was assumed as the hypothesis of preservative induced leveling where by the electrolyte additive(s) adsorb at the electrolyte-metal boundary, decreasing the energetic region and thus retarding the reduction procedure of metal. Given that the concentration of additive is diluted, the adsorption progression is characteristically considered to be limited by diffusion while the copper deposition process proceeds under interfacial charge-transfer control. In order to maintain the additives fluctuation, the adsorbate should moreover be incorporated in the mounting layer or go through decline desorption throughout deposition of metal. In the damascene progression, the channel outcomes in a lesser fluctuation of the diffusion to the features bottom than to the exterior outside [7,8]. Accordingly, the kinetics of metal deposition proceed extra quickly at the trench bottom that produce wonderful conformal substantial. This model also predicts that the slower growth occurs at the edge demarcating the entrance of the trench or *via* where the additives flux is expected to be greatest. However, it was essential to adjust the simple district-obstruction leveling hypothesis to facilitate imprison the investi-

gationally observed corner rounding and general shape change behaviour. The complexity of additive electrode interactions was recently highlighted by the observation of "overfill" where the originally concave surface profile becomes convex due to a sustained differential rate of metal deposition that cannot be rationalized by the transport-limited inhibition model outlined here. This observation has focused attention on the competition between species that accelerate *vs.* suppress deposition in the multi component additive packages [9,10].

Electropolishing and electrodeposition electrolytes usually contain a number of additives for various purposes. Some agents are used to increase electrolyte conductivity (supporting electrolytes). Others may be used for increasing bath stability (stabilizers), activating the surface (surfactants or wetting agents), improving levelling or metal distribution (levelling agents), or optimizing the chemical, physical or technology properties of the surface. These properties include corrosion resistance, brightness or reflectivity, hardness, mechanical strength, ductility, internal stress, wear resistance or solder ability [11-14].

Copper is extensively used in all kinds of industries because of its chemical, physical and mechanical properties. H_3PO_4 shows strong corrosiveness on copper and copper alloys. An immense require to save copper materials used in H_3PO_4 acid industry.

Plants are the sources of naturally occurring compounds, some with complex molecular structures and having different chemical, biological and physical properties. Different plant extracts can be used as dissolution inhibitors commonly known as green dissolution inhibitors. Green dissolution inhibitors are biodegradable and do not contain heavy metals or other toxic compounds [15-18]. Consequently, this study persists to spotlight on the purpose of biomass extracts for the electrochemical process and records the almond shell extract influence.

Almond, systematically recognized as *Prunus dulcis*, relates to Rosaceae family and is as well recountd to mineral crops like peaches, plums and cherries. Extracts of whole almond seed, brown skin and green shell cover possess potent free radical scavenging capacities [19-21]. In current study, the morphology investigation and particle size of electro copper powder from acidified copper sulfate solution is recorded and inspect the electropolishing process of copper in H_3PO_4 acid solution using potentiodynamic polarization measurements. Polished and deposited copper extent of were assessd *via* a featured investigation by different concentration of the almond shell extract influence.

EXPERIMENTAL

Equipments: Rectangular container with the dimensions of 5 cm × 10 cm × 15 cm used as cell in the present work, 5 cm × 10 cm × 0.2 cm test specimens copper electrodes which have the following content (wt.%): 0.0001 Cd, 0.001 Cd, 0.011 Ag, 0.003 Pb, 0.005 Sn and Cu is 99.98. 8 M H_3PO_4 (85% w/w) was used for electropolishing experiment while 0.15 M $CuSO_4 \cdot 5H_2O$, 1.5 M H_2SO_4 (98% w/w) for electrorefining experiments. The concentrations of almond shell extract cover range from 5 to 200 ppm.

Solution preparation: AnalaR grade chemicals (BDH chemicals Ltd.) were used for all trials, $CuSO_4$ and $Cu_3(PO_4)_2$ concentration were tested *via* iodometry procedure [22]. Demineralized water used in solutions preparation (resistivity > 18 mΩ).

Plant extract preparation: Almond shell (10 g) fine powder particles was weighed and boiled with double distilled water. The yellow solution was filtered to remove suspended contamination and made up to 100 mL. The almond shell extract was used as additives for polishing and refining bath in present study.

Experimental apparatus: The DC power supplier model 34 B DCPS (Testronix). The bath temperature stayed approximately steady throughout the trials (20, 30, 40 and 50 ± 1 ºC). Surface study was achieved *via* (JEOL, JSM-5300, scanning microscope, OXFORD instrument). Stylus profilometers (Talysurf i60) used to determine quantitative roughness The long cutoff wavelength (sampling) and the short cutoff wavelength were 0.25 mm and 0.025 mm, respectively. The evaluation length was 5 mm (five sampling lengths). Approximately 150 measuring lines were used. FTIR spectra were recorded on a Perkin-Elmer 1600 spectrophotometer.

RESULTS AND DISCUSSION

I-V curve and defining current process: A typical current-voltage (I-V) curve requires to be created through differing both electrolyte structure and temperature previous to electropolishing and electrorefining. An I-V plot (Fig. 1a-b) is constructed through changing voltage and designing it *versus* the electric current. The I-V plot determines whether the temperature and electrolyte amalgamation show a current flat terrain. The plateau of current is where altering in the voltage no longer persuade fluctuation in the progression current density, offering improved manage above the polishing and refining rate. Throughout electropolishing, H_2 gas are produced from the cathode while O_2 from anode [23]. The lower metal removal rate is the limiting aspect. Owing to electropolishing take places around 1 μm/min.

Owing to the less dispersion mechanism, a broad, sticky layer was sketched on the anode surface, which results in the delay of the electrochemical reaction, producing a current plateau on the I-V curve [24]. The anode surface polishing happens inside the thick sticky layer. Electropolishing in addition happens in the non-existence of the current plateau; however, owing to the current fluctuation, managed electropolishing may be difficult to achieve.

Effect of almond shell extract concentration: The interfacial mass transfer kinetics for copper electropolishing and refining procedure, potentiodynamic measurements were studied in free solution and solution containing extract. Clearly, a limiting current plateau could be found in each polarization curve. A perceptible augment in (I_L) for copper dissolution was observed when the almond shell extract was added (Table-1 and Fig. 1a).

Almond shell is lignocellulosic materials and the presence of oxygen atom as carbonyl group in the composition of almond shell as indicated by FTIR spectrum, which have a lone pair of electrons, there is a great probability for Cu^{2+} ions,

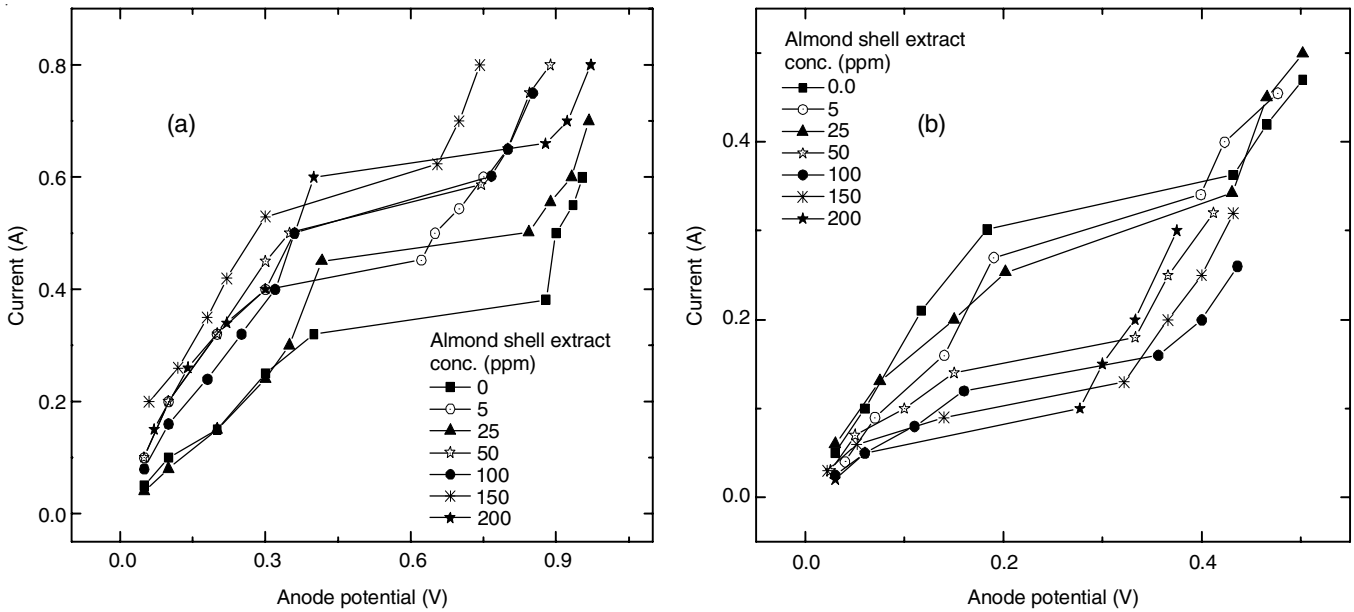

Fig. 1. Characteristic polarization plots for: (a) electropolishing in 8 M H_3PO_4, (b) electrorefining of vertical copper in attendance of several almond shell extract concentration at 20 °C

TABLE-1
LIMITING CURRENT VALUES, ACCELERATION % AND RETARDATION % FOR ELECTROPOLISHING AND REFINING OF COPPER IN THE PRESENCE OF DIFFERENT CONCENTRATION OF ALMOND SHELL EXTRACT

Conc. (ppm)	Electrodissolution								Electrodeposition							
	20 °C		30 °C		40 °C		50 °C		20 °C		30 °C		40 °C		50 °C	
	I_L (A)	AE (%)	I_L (A)	AE (%)	I_L (A)	AE (%)	I_L (A)	AE (%)	I_L (A)	AE (%)	I_L (A)	AE (%)	I_L (A)	AE (%)	I_L (A)	AE (%)
0	0.423	–	0.515	–	0.632	–	0.745	–	0.363	–	0.452		0.552	–	0.642	–
5	0.441	4.26	0.553	7.38	0.653	3.32	0.762	2.28	0.341	6.06	0.422	6.64	0.522	5.43	0.625	2.65
10	0.456	7.80	0.587	13.98	0.687	8.70	0.785	5.37	0.322	11.29	0.408	9.73	0.501	9.24	0.605	5.76
15	0.466	10.17	0.602	16.89	0.723	14.40	0.806	8.19	0.304	16.25	0.385	14.82	0.482	12.68	0.583	9.19
20	0.482	13.95	0.625	21.36	0.745	17.88	0.832	11.68	0.284	21.76	0.366	19.03	0.465	15.76	0.566	11.84
25	0.502	18.68	0.644	25.05	0.765	21.04	0.855	14.77	0.270	25.62	0.351	22.35	0.442	19.93	0.545	15.11
30	0.524	23.88	0.669	29.90	0.789	24.84	0.879	17.99	0.252	30.58	0.334	26.11	0.420	23.91	0.528	17.76
35	0.536	26.71	0.723	40.39	0.812	28.48	0.902	21.07	0.232	36.09	0.315	30.31	0.395	28.44	0.502	21.81
40	0.555	31.21	0.752	46.02	0.826	30.70	0.932	25.10	0.215	40.77	0.302	33.19	0.377	31.70	0.484	24.61
45	0.567	34.04	0.784	52.23	0.852	34.81	0.956	28.32	0.200	44.90	0.282	37.61	0.352	36.23	0.466	27.41
50	0.587	38.77	0.802	55.73	0.884	39.87	0.978	31.28	0.181	50.14	0.264	41.59	0.325	41.12	0.445	30.69
100	0.602	42.32	0.845	64.08	0.945	49.53	1.035	38.93	0.162	55.37	0.233	48.45	0.288	47.83	0.402	37.38
150	0.623	47.28	0.888	72.43	0.995	57.44	1.085	45.64	0.132	63.64	0.202	55.31	0.245	55.62	0.375	41.59
200	0.656	55.08	0.935	81.55	1.082	71.20	1.222	64.03	0.100	72.45	0.152	66.37	0.203	63.22	0.335	47.82

which produces through dissolution of copper metal, to interact or adsorb electrostatically on the oxygen lone pair by a sort of coordinate bond. The amount of Cu^{2+} ion decreases due to the formation of coordinate bond between Cu^{2+} ion and extract, *i.e.* more copper metal will dissolve and the rate of reaction increases. Therefore, it is concluded that the beneficial effect of almond shell extract is attributed to their interaction with Cu^{2+} ions. The performance of almond shell extracts has been ascribed to the strength of interaction with Cu^{2+} ions in solutions. The severity of the interaction depends upon the ease with which the heteroatom is able to donate the free electron pair. The acceleration % was calculated using eqn. 1:

$$\text{Acceleration } (\%) = \frac{I_{L(ASE)} - I_{L(BLANK)}}{I_{L(BLANK)}} \times 100 \qquad (1)$$

It was observed that acceleration % increases with increasing almond shell extracts concentration as represented in Fig. 2a. The contrasting behaviour was noticed for almond shell extract in electrorefining bath. It is observed that (I_L) was reduced as the concentration of the almond shell extract increase (Table-1 and Fig. 1b).

This performance may be explained as the almond shell extract metal surface interaction consequential in adsorption. The adsorption scope raises with the augment in the extract concentration directing to retardation effectiveness increase as shown in Fig. 2b. The suppressing capability of the extract instigates from the tendency to form which ever strapping or feeble chemical attachments with Cu atoms through the oxygen lone electrons pair and the benzene ring π-electrons. These organic molecules might adsorb on the metal/solution boundary

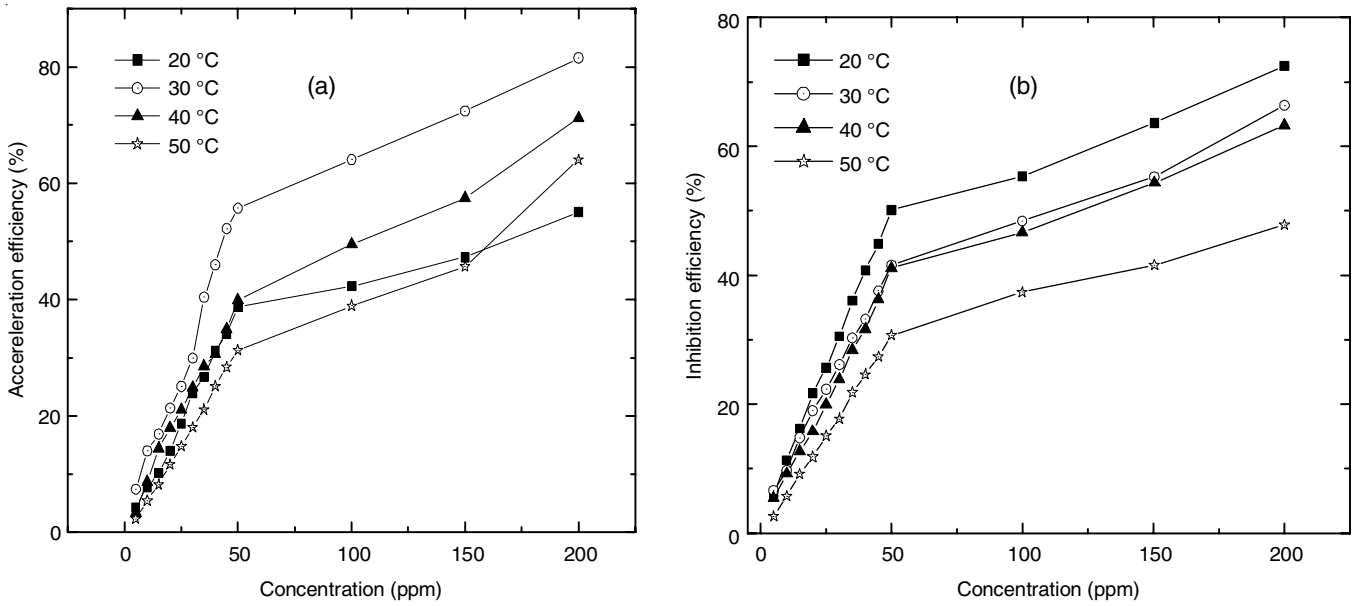

Fig. 2. (a) Acceleration effectiveness % as function of extract concentration plot at 20 °C, (b) inhibition effectiveness % as function of extract concentration plot at 20 °C

via one or more of the following methods; (i) the aromatic ring *p*-electrons vacant *d*-orbital copper metal interation (donor-acceptor interactions), (ii) unshared electron pairs of hetero-atoms copper vacant *d*-orbital interaction between [25]. Previous studies on the inhibitory effects of plant extracts are also reported [26-28]. These inhibition effects could result from an increase in the concentrations of the aromatic organic compounds within the plant extracts that promoted the formation of layers of varying complex organic compounds on the surface of the metal. It would also be in agreement with the expectation that larger amounts of inhibitor would be able to absorb onto a larger surface area of the metal and/or form a thicker layer of adsorbed molecules that could retard the refining process by coverage of active sites on the surface.The inhibition % was detrmined by applying the subsequent relationship:

$$\text{Inhibition } (\%) = \frac{I_{L(BLANK)} - I_{L(ASE)}}{I_{L(BLANK)}} \times 100 \quad (2)$$

Kinetic parameters: The discrepancy of the logarithm of the copper electrochemical process rate at 5, 25, 50, 100, 150 and g/L ASE *versus* 1/T was investigated (Fig. 3). It illustrates that the electrochemical reaction(polishing and refining) may be viewed as an Arrhenius-type process equation:

$$\ln I_L = -\left(\frac{E_a}{RT}\right) + \ln A \quad (3)$$

where the pre-exponential factor is A, that imitates the adsorption additives capacity on the metal surface, the reaction activation energy is E_a, the gas constant is R and T is the temperature.

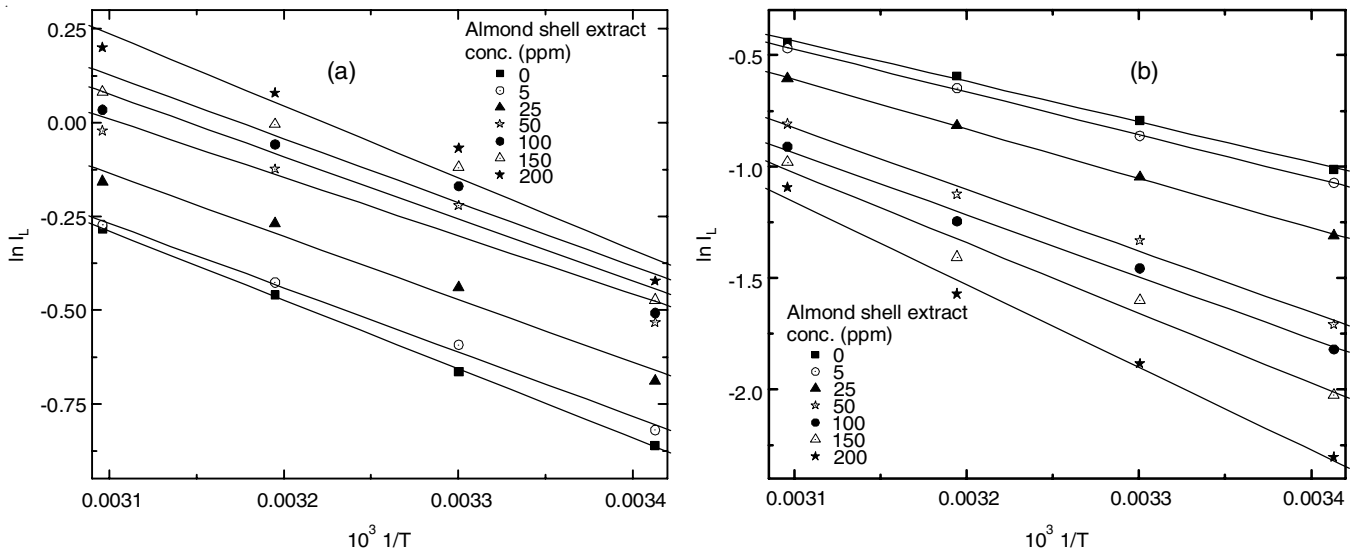

Fig. 3. Arrhenius curve for (a) copper dissolution & (b) copper refining in solution containing several concentration of almond shell extract

In present study, the activation energy (E_a) was found to be approximately 15.27 kJ/mol for blank electrodissolution progression while in solution containing 5, 25, 50, 100, 150 and 200 ppm ASE were 14.25, 14.13, 13.99, 13.80, 12.93 and kJ/mol, respectively. It is observed that E_a decreased in the presence of ASE. The lower E_a values are excellent confirmation of the strapping acceleration behaviour of ASE for the electrodissolution processes for copper metal. It is also noticed that E_a values decreases as ASE concentration increase, which confirmed that the acceleration performance of ASE is the concentration dependant.

While the activation energy (E_a) was approximately 15.07 kJ/mol for blank electrorefining processes while in the presence of 5, 25, 50, 100, 150 and 200 ppm ASE were 15.99, 18.42, 22.91, 23.14, 26.17 and 30.78 kJ/mol, respectively. Also, it is observed that activation energy (E_a) increases in solution containing ASE, which designates the deprived ASE recital at the elevated temperature. The activation energy augment is usually illustrated through ASE-Cu surface electrostatic adsorption process and ASE contents being adsorbed on the copper surface in physically style [29-31].

The activation parameters ($\Delta H^{\#}$, $\Delta S^{\#}$ and $\Delta G^{\#}$) were computed *via* the transition state approach [32]:

$$I_L = \frac{RT}{Nh}\exp\left(\frac{\Delta S^{\#}}{R}\right)\exp\left(-\frac{\Delta H^{\#}}{RT}\right) \quad (4)$$

$$\Delta G^{\#} = \Delta H^{\#} - T\Delta S^{\#} \quad (5)$$

where the h = Plank's constant, N = Avogadro's number, $\Delta H^{\#}$ = activation enthalpy, $\Delta S^{\#}$ = activation entropy and $\Delta G^{\#}$ = activation free energy. The activation parameters data represented in Table-2, which concluded that (i) positive ΔH values reflect the copper dissolution and refining processes is endothermic in nature [33]; (ii) negative $\Delta S^{\#}$ values entailed that the rate determining step, the activated complex signifies an organization rather than separation. *i.e.* threre is a dimish in disordering occured on the reactants to the activated complex transfer [34]; (iii) $\Delta G^{\#}$ values in solution containing ASE were more positive than free solution in electrorefining procedure designated in the presence of ASE, the activated complex develop into fewer stable in comparison to its free solution in contrast for electro-dissolution, the free ASE solution has more positive value of $\Delta G^{\#}$ than ASE containing solution, which reflect that the activated complex in ASE containing solution is more stable.

Adsorption isotherm: In sequence to know more information around the almond shell extract adsorption mode on the copper surface, the investigational statistics have been inspected with the next two adsorption isotherms. The representative Langmuir adsorption plot was obtained at 20 ºC with various concentrations of almond shell extract which is shown in Fig. 4a. The linear curve has the value of slope equal to 1.07. These results could also indicate that the extract of almond shell occupied one adsorption site on the copper surface in the electrorefining process [35,36].

Plotting log θ/1-θ *versus* log C for almond shell extract at 20 ºC (Fig. 4b), the linear-correlation can be attained. It was observed that the *y*-values equal one value and confirmed that the extract of almond shell occupied one adsorption site on the copper surface in the electrorefining process [37].

Langmuir:

$$\frac{C}{\theta} = \frac{1}{K} + C \quad (6)$$

Kinetic-thermodynamic:

$$(KC)^{Y} = \left(\frac{\theta}{1-\theta}\right) \quad (7)$$

Analysis of copper surface using SEM: The surface texture morphology was patently influenced by the concentration of ASE. Fig. 5a shows the electrodeposited copper morphology in acidified copper sulfate for 5 min at 20 ºC. Copper particles essentially exist as cauliflower-akin to construction. A permeable canal arrangement throughout that the powder particle interior may be observed. Copper bath containing ASE revealed a strapping manipulate on the microconstruction *i.e.* deposit sanitization (Fig. 5b-d) *via* mounting its concentration the deposit appear is powerfully supporter and consistently wraps the complete electrode surface. In these circumstances, enlargement is beneath nucleation manage *via* dischargeable species adsorption, undermine the bottom imitation enlargement manner. Surface chunking directs to the progress of a unimaginative morphology, through whole repression of privileged augmentation of isolated crystals in the premature phases of deposition, promoting structure refinement and surface levelling.

Surface morphology was also inspected on the electropolished sample at 20 ºC for 5 min. Fig. 6a represents the copper morphology before electropolishing. Each pits were found with huge dimension and elevated deepness allocated above the surface are shown. In contrast, after electropolishing in 8 M

TABLE-2
ACTIVATED PARAMETERS VALUES FOR ELECTROPOLISHING AND REFINING OF COPPER IN SOLUTION CONTAING SEVERAL ALMOND SHELL EXTRACT CONCENTRATION

Conc. (ppm)	Electrodissolution (Electropolishing)				Electrodeposition			
	E_a (kJ mol^{-1})	ΔH^* (kJ mol^{-1})	$-\Delta S^*$ (J mol^{-1} K^{-1})	$-\Delta G^*$ (kJ mol^{-1})	E_a (kJ mol^{-1})	ΔH^* (kJ mol^{-1})	$-\Delta S^*$ (J mol^{-1} K^{-1})	$-\Delta G^*$ (kJ mol^{-1})
0	15.27	11.78	208.31	74.90	15.07	12.59	210.16	75.25
5	14.25	12.79	211.27	74.77	15.99	13.52	207.60	75.41
25	14.13	11.65	210.96	74.41	18.42	15.94	201.20	75.93
50	13.99	10.52	213.08	73.98	22.91	20.43	189.11	76.81
100	13.80	11.45	209.82	73.88	23.14	20.66	189.30	77.10
150	12.93	11.35	208.36	73.78	26.17	23.69	180.66	77.56
200	12.80	11.48	201.8	73.64	30.78	28.30	167.48	78.24

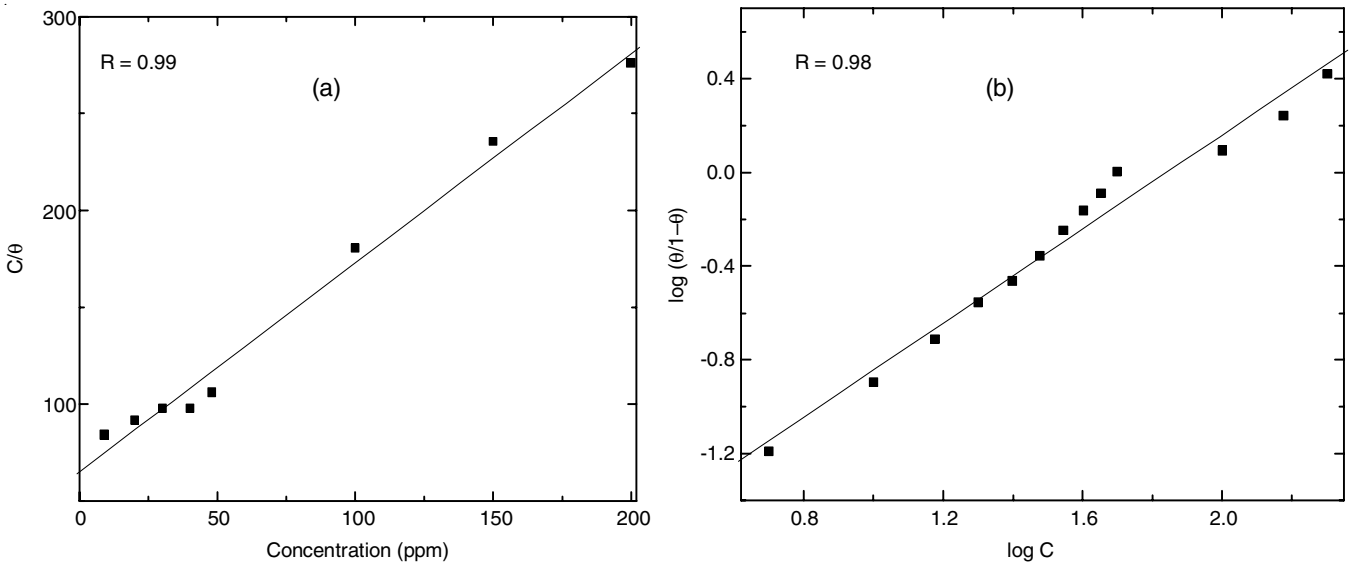

Fig. 4. (a) Langmuir isotherm (b) Kinetic-thermodynamic adsorption isotherms for refining process in the presence of different concentration of almond shell extract

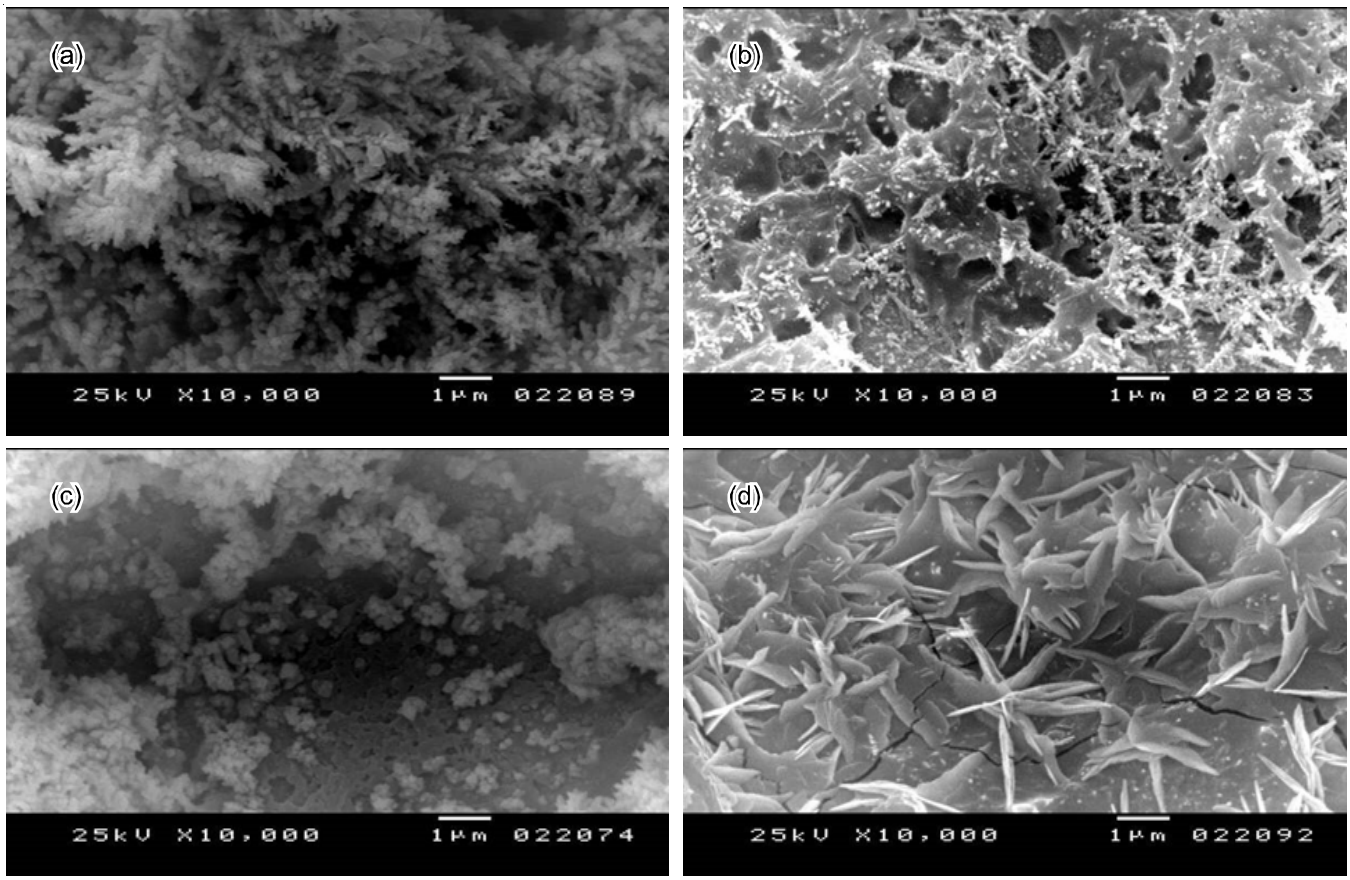

Fig. 5. (a) Blank of copper, (b) After ER + 25 ppm ASE, (c) After ER + 100 ppm ASE (d) After ER + 200 ppm ASE

H_3PO_4, a smooth surface without major defects, the grain structures were observed (Fig. 6b). Inspection of Fig. 6c-e, it is observed that a gradual increase in surface quality and uniformity by increasing the concentration of ASE of 25-200 ppm at 20 ºC, the surface was well polished, smooth and completely uniform but by increasing concentration of 200 ppm, leveling and brightening results were noticeably improved by the addition of ASE, where ASE is satisfied up the channels and grain boundaries, as well etching influence were eradicated.

Surface roughness: The surface roughness decreased with an increase in ASE concentration, for a raw copper material, an average surface roughness was 0.94 nm. The surface roughness decreased to 0.63 nm after polishing in 8 M H_3PO_4. From Table-3, the surface roughness will be reduced by addition of

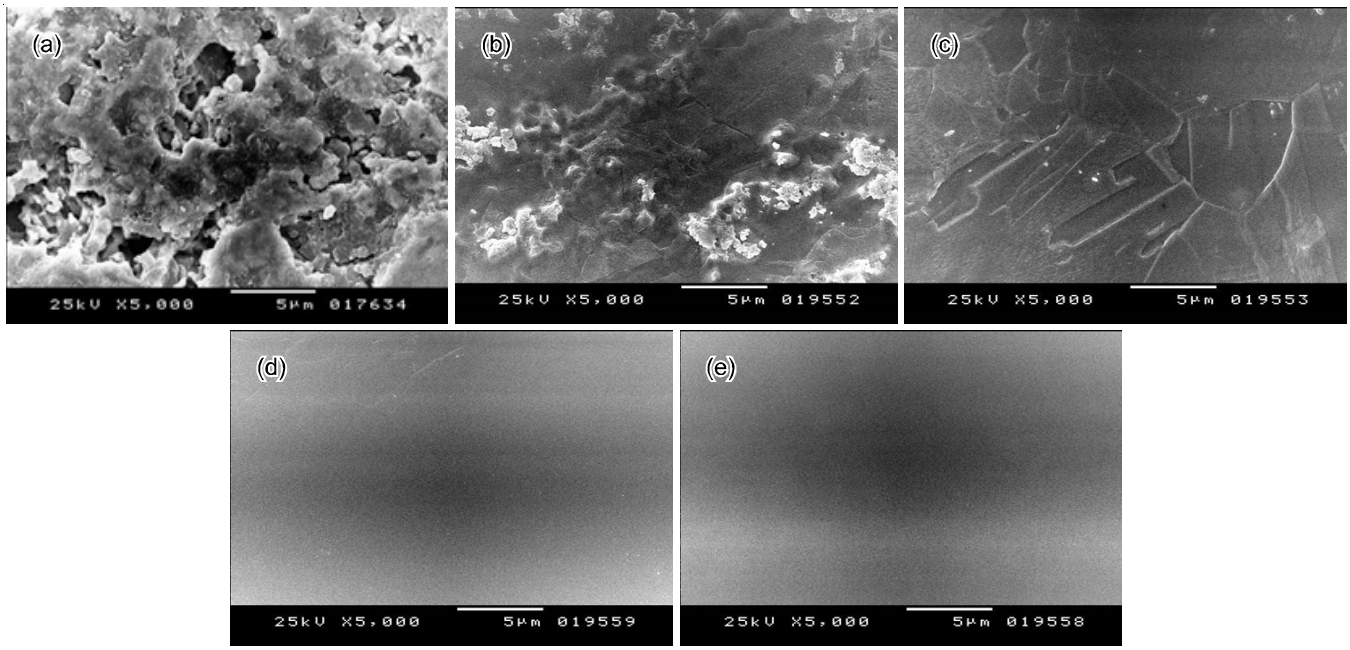

Fig. 6. (a) Raw material of copper, (b) after electropolishing without addition (blank), (c) after electropolishing + 25 ppm ASE, (d) after electropolishing + 100 ppm ASE, (e) after electropolishing + 200 ppm ASE

TABLE-3
MEASURED ROUGHNESS (Ra), Rq (RMS), Rz AND PEAK VALLEY (PV) RATIO OF COPPER SAMPLES

ASE conc. (ppm)	Raw sample	0.00	25	100	150	200
Ra (µm)	0.95	0.63	0.43	0.32	0.22	0.06
Rq (µm)	2.55	0.82	0.74	0.52	0.36	0.16
Rz (µm)	3.80	2.15	1.42	1.26	0.84	0.42
PV (µm)	30.00	8.35	3.45	3.00	1.88	1.43

different concentration of ASE. The The roughness (Ra) values decreases to 0.43, 0.32, 0.22 and 0.06 µm in the presence of 25, 100, 150 and 200 ppm (Table-3).

The surface roughness reduce may be interpreted *via* the electropolishing infulence. When the current was applied to the anode and anode potential develop into superior at the current flat terrain, elevated specific gravity, extremely thick and insulate anodic layer wrap a surface. The anodic layer wraps the inferior crests and basins avoiding dissolution; while elevated values with elevated charge concentration are projected over the anodic layers dissolve more readily [38]. In combination, more material surface was removed with an augment in electropolishing time, as assumed from Faraday's law of electrolysis

An increase in the surface roughness on blank samples may have owed to the same procedure current, which was observed at the I-V curve base with low anode potential. Owing to the small anode potentials, the shielding anodic film failed to outline on the sample surface which should have avoided the material dissolution from low crests and valleys [38]. The surface was etched when the anode potential was small, which may increase in the surface roughness when the sample were electropolished at the lowest current.

FTIR analysis: Fig. 7 shows the FTIR spectrum of almond shells. The peaks exhibited the major adsorption bands at 3432.13 (-O-H *str.*), 2926.10 (C–H arom.), 1739.35, 1635.19 (C=O *str.*), 1461, 1430, 1378.02 (C–H *def.*), 1252.28, 1110, 1052.28 (C–O *str.*) and 668.76 cm^{-1} (SiO–H *str.*).

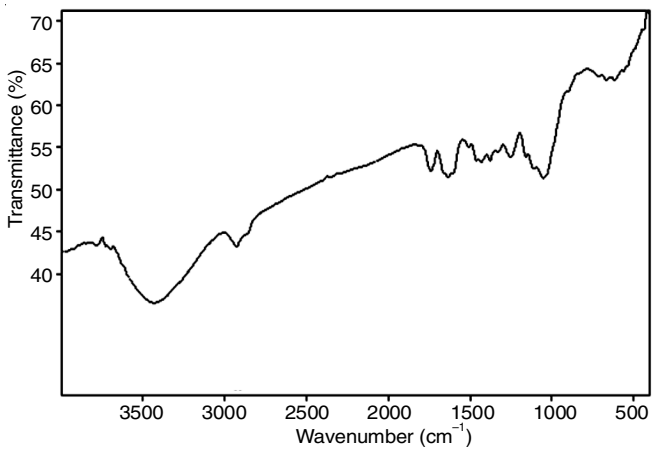

Fig. 7. FTIR spectrum of almond shells

Conclusion

In this work, potentiodynamic polarization results indicate that the addition of almond shell extract leades to increase in the rate of electropolishing other than reduce the rate of electrorefining of copper. The electropolishing and electrorefining behaviour of the copper surface was significantly affected by concentration of the almond shell extract. According to SEM, addition of high concentration of almond shell extract to the electrolytic solution was extremely successful to improve surface excellence for deposited and polished copper. The roughness (Ra) values designated that electropolished

copper surface is more successful solution containing almond shell extract (Ra = 0.06 μm).

CONFLICT OF INTEREST

The authors declare that there is no conflict of interests regarding the publication of this article.

REFERENCES

1. G. Yang, B. Wang, K. Tawfiq, H. Wei, S. Zhou and G. Chen, *Surf. Eng.*, **33**, 149 (2017); https://doi.org/10.1080/02670844.2016.1198452
2. T. Hryniewicz, K. Rokosz and H.R.Z. Sandim, *Appl. Surf. Sci.*, **263**, 357 (2012); https://doi.org/10.1016/j.apsusc.2012.09.060
3. X. Wang, C. Li, Z. Yu, H. Zheng, Y. Ji, P. Ji, Z. Chen and Z. Fan, *Mater. Chem. Phys.*, **133**, 212 (2012); https://doi.org/10.1016/j.matchemphys.2012.01.010
4. W. Simka, M. Mosialek, G. Nawrat, P. Nowak, J. Zak, J. Szade, A. Winiarski, A. Maciej and L. Szyk-Warszynska, *Surf. Coat. Technol.*, **213**, 239 (2012); https://doi.org/10.1016/j.surfcoat.2012.10.055
5. M. Schlesingera and M. Paunovic, Modern Electroplating, Wiley: New York, Ed. 4 (2000).
6. A. Radisic, J.G. Long, P.M. Hoffmann and P.C. Searson, *J. Electrochem. Soc.*, **148**, 41 (2001); https://doi.org/10.1149/1.1344539
7. G. Oskam, P.M. Vereecken and P.C. Searson, *J. Electrochem. Soc.*, **146**, 1436 (1999); https://doi.org/10.1149/1.1391782
8. T.P. Moffat, B. Baker, D. Wheeler, J.E. Bonevich, M. Edelstein, D.R. Kelly, L. Gan, G.R. Stafford, P.J. Chen, W.F. Egelhoff and D. Josell, *J. Electrochem. Soc.*, **149**, 423 (2002); https://doi.org/10.1149/1.1490357
9. A. Ramos, M. Miranda-Hernández and I. González, *J. Electrochem. Soc.*, **148**, 315 (2001); https://doi.org/10.1149/1.1357176
10. C. Nila and I. González, *J. Electroanal. Chem.*, **401**, 171 (1996); https://doi.org/10.1016/0022-0728(95)04278-4
11. M. Christophersen, J. Carstensen, K. Voigt and H. Föll, *Phys. Status Solid.*, **197**, 34 (2003); https://doi.org/10.1002/pssa.200306464
12. O. Piotrowski, C. Madore and D. Landolt, *J. Electrochem. Soc.*, **145**, 2362 (1998); https://doi.org/10.1149/1.1838644
13. S.J. Lee and J.J. Lai, *J. Mater. Process. Technol.*, **140**, 206 (2003); https://doi.org/10.1016/S0924-0136(03)00785-4
14. P. Kao and H. Hocheng, *J. Mater. Process. Technol.*, **140**, 255 (2003); https://doi.org/10.1016/S0924-0136(03)00747-7
15. A.A. Taha, F.M. Abouzeid, M.M. Elsadek and F.M. Habib, *Arab. J. Chem.*, **13**, 6606 (2020); https://doi.org/10.1016/j.arabjc.2020.06.017
16. A.S. Fouda, Y.M. Abdallah, G.Y. Elawady and R. Ahmed, *Int. J. Adv. Res.*, **2**, 517 (2014).
17. C.O. Akalezi, C.K. Enenebaku and E.E. Oguzie, *Int. J. Ind. Chem.*, **3**, 13 (2012); https://doi.org/10.1186/2228-5547-3-13
18. H. Bouammali, A. Ousslim, K. Bekkouch, B. Bouammali, A. Aouniti, S.S. Al-Deyab, C. Jama, F. Bentiss and B. Hammouti, *Int. J. Electrochem. Sci.*, **8**, 6005 (2013).
19. A.J. Sfahlan, A. Mahmoodzadeh, A. Hasanzadeh, R. Heidari and R. Jamei, *Food Chem.*, **115**, 529 (2009); https://doi.org/10.1016/j.foodchem.2008.12.049
20. S. Siriwardhana and F. Shahidi, *J. Am. Oil Chem. Soc.*, **79**, 903 (2002); https://doi.org/10.1007/s11746-002-0577-4
21. G. Takeoka, L. Dao, R. Teranishi, R. Wong, S. Flessa, L. Harden and R. Edwards, *J. Agric. Food Chem.*, **48**, 3437 (2000); https://doi.org/10.1021/jf9908289
22. J. Mendham, R.C. Denney and M.B. Thomas, Vogel's Quantitative Chemical Analysis, Ed. 6 (2004).
23. M. Cabibbo, H.J. McQueen, E. Evangelista, S. Spigarelli, M. Di Paola and A. Falchero, *Mater. Sci. Eng. A*, **460–461**, 86 (2007); https://doi.org/10.1016/j.msea.2007.01.022
24. J.H. Potgieter, P.A. Olubambi and N.P. Thanjekwayo, *J. Metallur. Eng.*, **1**, 41 (2012).
25. K.O. Orubite and N.C. Oforka, *Mater. Lett.*, **58**, 1768 (2004); https://doi.org/10.1016/j.matlet.2003.11.030
26. A.Y. El-Etre, M. Abdallah and Z.E. El-Tantawy, *Corros. Sci.*, **47**, 385 (2005); https://doi.org/10.1016/j.corsci.2004.06.006
27. L.R. Chauhan and G. Gunasekaran, *Corros. Sci.*, **49**, 1143 (2007); https://doi.org/10.1016/j.corsci.2006.08.012
28. L. Afia, R. Salghi, L. Bammou, Lh. Bazzi, B. Hammouti and L. Bazzi, *Acta Metall. Sin.*, **25**, 10 (2012).
29. M. Elayyachy, A. El Idrissi and B. Hammouti, *Corros. Sci.*, **48**, 2470 (2006); https://doi.org/10.1016/j.corsci.2005.09.016
30. H.P. Sachin, M.H. Moinuddin Khan and N.S. Bhujangaiah, *Int. J. Electrochem. Sci.*, **4**, 134 (2009).
31. A.A. Taha, H.H. Abdel Rahman and F.M. Abouzeid, *Int. J. Electrochem. Sci.*, **8**, 6744 (2013).
32. F.M. Abouzeid, *Asian J. Chem.*, **28**, 743 (2016); https://doi.org/10.14233/ajchem.2016.19418
33. O. Krim, A. Elidrissi, B. Hammouti, A. Ouslim and M. Benkaddour, *Chem. Eng. Commun.*, **196**, 1536 (2009); https://doi.org/10.1080/00986440903155451
34. N.S. Patel, S. Jauharian, G.N. Mehta, S.S. Al-Deyab, I. Warad and B. Hammouti, *Int. J. Electrochem. Sci.*, **8**, 2635 (2013).
35. M. Abdallah, *Corros. Sci.*, **46**, 1981 (2004); https://doi.org/10.1016/j.corsci.2003.09.031
36. I.M. Iloamaeke, T.U. Onuegbu, U.C. Umeobika and N.L. Umedum, *Int. J. Sci. Modern Eng.*, **1**, 48 (2013).
37. A.Y. El-Etre, *Corros. Sci.*, **45**, 2485 (2003); https://doi.org/10.1016/S0010-938X(03)00066-0
38. F.M. Abouzeid and H.A. Abubshait, *Arab. J. Chem.*, **13**, 2579 (2020); https://doi.org/10.1016/j.arabjc.2018.06.011